DOI: 10.1002/ejic.200600944

Syntheses, Characterization and Reactivity of Iron(II), Nickel(II), Copper(II) and Zinc(II) Complexes of the Ligand *N*,*N*,*N*′,*N*′-Tetrakis(2-pyridylmethyl)-benzene-1,3-diamine (1,3-tpbd) and Its Phenol Derivative 2,6-Bis[bis(2-pyridylmethyl)amino]-*p*-cresol (2,6-tpcd)

Simon Foxon,[a,b] Jing-Yuan Xu,[a,c] Sabrina Turba,[a] Michael Leibold,[d,e] Frank Hampel,[f] Frank W. Heinemann,[g] Olaf Walter,[d] Christian Würtele,[a] Max Holthausen,[h] and Siegfried Schindler*[a]

Keywords: Iron / Copper / Zinc / Ligand effects

N,*N*,*N*′,*N*′-Tetrakis(2-pyridylmethyl)benzene-1,3-diamine (1,3-tpbd), a bis(tridentate) ligand, its protonated derivative, [1,3-tpbdH$_2$]$^{2+}$, and a series of new dinuclear complexes [Fe$_2$(1,3-tpbd)(CH$_3$CN)$_6$](ClO$_4$)$_4$·(CH$_3$CN)$_2$·(H$_2$O)$_{0.5}$ (**1**), [Fe$_2$(1,3-tpbd)(DMF)$_6$](ClO$_4$)$_4$ (**2**), [Ni$_2$(1,3-tpbd)(DMF)$_6$](ClO$_4$)$_4$ (**3**), [Zn$_2$(1,3-tpbd)(CH$_3$CN)$_2$(SO$_3$CF$_3$)$_2$(H$_2$O)](SO$_3$CF$_3$)$_2$ (**4**), [Zn$_2$(1,3-tpbd)Cl$_4$]·H$_2$O (**5**), [CuZn(1,3-tpbd)Cl$_4$] (**7**) and the tetranuclear copper(II) complex [Cu$_2$(1,3-tpbd)$_2$(H$_2$O)$_2$](ClO$_4$)$_4$·2H$_2$O (**8**) have been prepared and structurally characterized. Complex **8**, a so called "dimetallocyclophane", interestingly only formed in the presence of zinc ions and not when copper(II) ions were mixed stoichiometrically (1:1 mixtures) under aerobic conditions. Theoretical calculations provide evidence for the formation of a side-on dinuclear peroxido copper complex during the oxidation of the (1,3-tpbd)copper(I) complex. A possible reaction product, the dinuclear copper complex [Cu$_2$(2,6-tpcd)(H$_2$O)(Cl)](ClO$_4$)$_2$·2H$_2$O (**9**) of a phenolate derivative of 1,3-tpbd was synthesized and structurally characterized independently from oxidation reactions from copper(II) perchlorate and the ligand 2,6-bis[bis(2-pyridylmethyl)amino]-*p*-cresol.

Introduction

Previously we have demonstrated that the ligand *N*,*N*,*N*′,*N*′-tetrakis(2-pyridylmethyl)benzene-1,3-diamine (1,3-tpbd) shown in Figure 1 can coordinate two copper ions in close proximity.[1–3] In this regard copper complexes of 1,3-tpbd or its phenol derivative 2,6-bis[bis(2-pyridylmethyl)-amino]-*p*-cresol (2,6-tpcd) (Figure 1) represent good structural models of the histidine-rich environments found in many dinuclear copper proteins (such as *hemocyanin and tyrosinase*).[1,4–7]

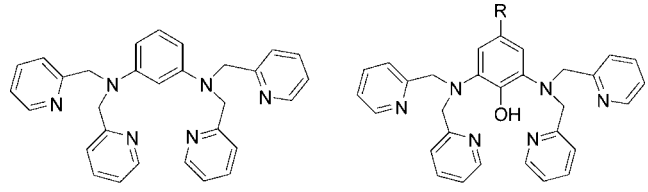

1,3-tpbd **2,6-tpcd**

Figure 1. The ligands *N*,*N*,*N*′,*N*′-tetrakis(2-pyridylmethyl)benzene-1,3-diamine (1,3-tpbd) and 2,6-bis[bis(2-pyridylmethyl)amino]-*p*-cresol (2,6-tpcd; R = CH$_3$).

Furthermore, the intramolecular magnetic coupling observed in a series of copper(II) complexes with 1,3-tpbd could be tuned from ferromagnetic to antiferromagnetic.[2,3] Similar ferromagnetic coupling has been observed for copper complexes with a related *m*-phenylenediamine-based ligand system.[8,9] Recently, a 1,3-tpbd platinum complex has been used in mechanistic studies.[10] However to date, only

[a] Institut für Anorganische und Analytische Chemie, Justus-Liebig-Universität Gießen,
Heinrich-Buff-Ring 58, 35392 Gießen, Germany
Fax: +49-641-9934149
E-mail: siegfried.schindler@chemie.uni-giessen.de
[b] Department of Chemistry, University of Sheffield, Sheffield, S3 7HF, United Kingdom
[c] College of Pharmacy, Tianjiin Medical University, 300070 Tianjiin, China
[d] Institut für Technische Chemie – Chemisch-Physikalische Verfahren (ITC-CPV), Forschungszentrum Karlsruhe, Postfach 3640, 76021 Karlsruhe, Germany
[e] Fachbereich Metallorganische Chemie, Universität Kassel, Heinrich-Plett-Strasse 40, 34132 Kassel, Germany
[f] Institut für Organische Chemie, Friedrich-Alexander-Universität Erlangen-Nürnberg, Henkestrasse 42, 91054 Erlangen, Germany
[g] Institut für Anorganische Chemie, Friedrich-Alexander-Universität Erlangen-Nürnberg, Egerlandstrasse 1, 91058 Erlangen, Germany
[h] Institut für Anorganische und Analytische Chemie, Johann-Wolfgang-Goethe-Universität Frankfurt/Main, Max-von-Laue-Strasse 7, 60438 Frankfurt, Germany
Supporting information for this article is available on the WWW under http://www.eurjic.org or from the author.

a small number of transition-metal complexes of related derivatives of the 1,3-tpbd ligand system have been investigated.[11–21]

To gain further understanding of the ligating ability of 1,3-tpbd, we herein describe the synthesis and characterization of a series of iron(II), zinc(II) and copper(II) complexes with 1,3-tpbd as well as a copper(II) complex of the phenol analogue of 1,3-tpbd. A similar complex with the phenol derivative ligand shown in Figure 1 (R = *tert*-butyl) and its interesting properties (e.g. interactions with DNA) was recently reported by Karlin and co-workers.[15,16]

Results and Discussion

***N*,*N*,*N*′,*N*′-Tetrakis(2-pyridylmethyl)benzene-1,3-diamine (1,3-tpbd):** 1,3-tpbd was prepared in modest yields from commercially available *m*-phenylenediamine and picolyl chloride hydrochloride as previously reported.[1] Single crystals of 1,3-tpbd, suitable for structural characterization, were obtained by slow evaporation of a methanol solution of 1,3-tpbd in a glove box. Attempts to recrystallize the ligand outside of the glovebox often caused the formation of nearly colorless crystals in a slightly brown mother liquor. The solution turned to an intense red color during a couple of days affecting the crystals as well (most likely the ligand is partially oxidized) and as a consequence numerous attempts to solve the crystal structure failed due to poor refinement. A summary of crystal structure data and refinement parameters is presented in Table 2, selected bond lengths and angles in Table 1. The molecular structure of 1,3-tpbd is shown in Figure 2. The two pyridyl units bonded at each amine nitrogen atom are separated from each other by a large distance similar to the previously reported molecular structure of 1,4-tpbd.[18] 1,3-tpbd crystallizes with one additional methanol solvent molecule per unit, hydroxyl hydrogen atom of the methanol solvent molecule were located in a difference Fourier map and isotropically refined.

Protonation of 1,3-tpbd or coordination of 1,3-tpbd to metal ions has the consequence that the pyridyl units move much closer together. In Figure 3 the molecular structure of the cation of $[1,3\text{-tpbdH}_2](ClO_4)_2$ is shown (crystal structure data and refinement parameters, bond lengths and angles are presented in Table 2 and Table 1).

$[1,3\text{-tpbdH}_2](ClO_4)_2$ crystallizes with two molecules per crystallographically independent unit of the unit cell together with three molecules of acetonitrile. Two of the ClO_4^- anions are disordered. The H atoms of the protonated N atoms were localized in a difference Fourier map and refined isotropically. The crystal structures of 1,3-tpbd and $[1,3\text{-tpbdH}_2]^{2+}$ display similar metrical parameters. The immediate geometry around the aliphatic amine nitrogen atoms is nearly planar with C1–N1 1.388(2) Å in 1,3-tpbd and C13–N1 1.396(4) Å in $[1,3\text{-tpbdH}_2](ClO_4)_2$ indicating delocalization of the nitrogen lone pair of electrons with the aromatic π systems. All the interbond angles around the aliphatic amine nitrogen atoms are close to 120°. However, as discussed above, the positions of the pyridine rings in 1,3-tpbd and its protonated derivative are quite different. In $[1,3\text{-tpbdH}_2]^{2+}$ adjacent pyridine nitrogen atoms on each ligand "arm" [N2 and N3, N5 and N6] are strongly hydrogen-bonded to one another. The average distance between the hydrogen-bonded pyridine nitrogen atoms is 2.741 Å. Additionally, we obtained the protonated triflate salt of 1,3-tpbd (see Supporting Information; for Supporting Information see also the footnote on the first page of this paper) of which the cation is identical to $[1,3\text{-tpbdH}_2](ClO_4)_2$. However, the two crystal structures differ from each other due to the crystal-packing arrangement of the anions, and furthermore the inclusion of additional solvent molecules. In principle these protonated ligand salts are comparable to the metal complexes (see below) and the protons in $[1,3\text{-tpbdH}_2]^{2+}$ can be regarded as small metal cations. The previously reported crystal structure of $[1,4\text{-tpbdH}_2]^{2+}$ displays similar bond lengths and angles to the $[1,3\text{-tpbdH}_2]^{2+}$ structure described above.[18]

Iron Complexes: Ligands capable of coordinating two iron ions in close proximity have been employed as structural models for dinuclear iron metalloproteins (e.g. the oxygen carrier protein hemerythrin).[22–24] Prior to the investigations of the oxygen-sensitive iron(II) model compounds, we tried to synthesize and structurally characterize an iron(III) complex of 1,3-tpbd. However, all our efforts to date in obtaining an 1,3-tpbd iron(III) complex were unsuccessful. Numerous attempts (employing different reaction conditions) to synthesize $[Fe_2(1,3\text{-tpbd})]^{6+}$ derivatives, such as $[Fe_2(1,3\text{-tpbd})(DMF)_6]^{6+}$ or $[Fe_2(1,3\text{-tpbd})(RCOO)_n]^{(6-n)+}$, by the reaction of 1,3-tpbd with $Fe(ClO_4)_3$ in different solvents (coordinating or non-coordinating), with and without addition of anions such as AsO_4^{3-}, $C_6H_5COO^-$, CH_3COO^- or Cl^-, only afforded the protonated free ligand and unreacted iron salts. Over a period of weeks single crystals, suitable for X-ray structural analysis, of $[1,3\text{-tpbdH}_2](SO_3CF_3)_2$ (see supp. inf. and Experimental Section) and $[1,3\text{-tpbdH}_2](ClO_4)_2$ described above (Figure 3) were obtained. Furthermore, efforts in obtaining an 1,3-tpbd iron(III) complex by oxidizing the corresponding iron(II) precursor complex (described below) failed. These results clearly indicate that the 1,3-tpbd ligand has a low affinity for iron(III). In the presence of water, protonation of the ligand occurs, however in the absence of protons no complexation of the iron(III) ions was observed either. Other pyridyl containing ligands are known to stabilize iron(II) relative to iron(III), however in these cases it was still possible to synthesize, isolate and characterize the according iron(III) complexes.[25]

An iron(II) complex of 1,3-tpbd was prepared and single crystals of $[Fe_2(1,3\text{-tpbd})(CH_3CN)_6](ClO_4)_4{\cdot}2CH_3CN{\cdot}0.5H_2O$ (**1**) were grown. The molecular structure of the cation $[Fe_2(1,3\text{-tpbd})(CH_3CN)_6]^{4+}$ of **1** is shown in Figure 4 (crystal structure data and refinement parameters, bond lengths and angles are presented in Table 2 and Table 1). The unit cell of **1** consists of two sets of crystallographically independent dinuclear cations, $[Fe_2(1,3\text{-tpbd})(CH_3CN)_6]^{4+}$,

Table 1. Selected bond lengths [Å] and angles [°] for 1,3-tpbd ligand and compounds **1**–**9**.

1,3-tpbd					
N(1)–C(1)	1.411(2)	N(5)–C(24)	1.326(4)	C(1)–N(1)–C(7)	120.7(2)
N(1)–C(7)	1.451(2)	N(5)–C(20)	1.336(2)	C(1)–N(1)–C(13)	118.5(2)
N(1)–C(13)	1.460(2)	N(6)–C(30)	1.333(3)	C(7)–N(1)–C(13)	115.1(2)
N(2)–C(8)	1.345(2)	N(6)–C(26)	1.339(2)	C(8)–N(2)–C(12)	117.2(2)
N(2)–C(12)	1.357(3)	C(7)–C(8)	1.514(3)	C(18)–N(3)–C(14)	117.2(2)
N(3)–C(18)	1.342(3)	C(8)–C(9)	1.382(3)	C(3)–N(4)–C(19)	121.4(2)
N(3)–C(14)	1.348(2)	C(9)–C(10)	1.381(3)	C(3)–N(4)–C(25)	120.4(2)
N(4)–C(3)	1.388(2)	C(10)–C(11)	1.370(3)	C(19)–N(4)–C(25)	117.9(2)
N(4)–C(19)	1.452(2)	C(11)–C(12)	1.371(4)	C(24)–N(5)–C(20)	117.1(2)
N(4)–C(25)	1.454(2)			C(30)–N(6)–C(26)	117.1(2)
$[H_2$1,3-tpbd$](ClO_4)_2$					
N(2)–H(2A)	0.84(4)	N(3)–C(8)	1.336(4)	C(13)–N(1)–C(1)	119.8(2)
N(5)–H(5A)	0.94(4)	N(3)–C(12)	1.343(4)	C(1)–N(1)–C(7)	118.6(2)
N(1)–C(13)	1.396(4)	C(7)–C(8)	1.517(4)	C(13)–N(1)–C(7)	119.7(2)
N(1)–C(1)	1.449(4)	C(8)–C(9)	1.386(5)	C(17)–N(4)–C(19)	121.3(2)
N(1)–C(7)	1.453(4)	C(9)–C(10)	1.388(6)	C(17)–N(4)–C(25)	119.6(2)
N(2)–C(6)	1.340(4)	N(4)–C(17)	1.397(4)	C(19)–N(4)–C(25)	118.8(2)
N(2)–C(2)	1.348(4)	N(4)–C(19)	1.447(4)	C(6)–N(2)–H(2A)	120(3)
C(1)–C(2)	1.514(4)	N(4)–C(25)	1.451(4)	C(2)–N(2)–H(2A)	118(3)
C(2)–C(3)	1.378(4)	N(5)–C(20)	1.334(4)	C(24)–N(5)–H(5A)	121(2)
C(3)–C(4)	1.388(5)	N(5)–C(24)	1.341(5)	C(20)–N(5)–H(5A)	116(2)
C(4)–C(5)	1.372(6)	N(6)–C(26)	1.337(5)		
C(5)–C(6)	1.372(5)	N(6)–C(30)	1.352(5)		
$[Fe_2$(1,3-tpbd)$(CH_3CN)_6](ClO_4)_4 \cdot 2CH_3CN \cdot 0.5H_2O$ (**1**)					
Fe(1)–N(3)	1.989(3)	N(3)–Fe(1)–N(9)	171.8(2)	N(11)–Fe(2)–N(6)	168.6(1)
Fe(1)–N(9)	1.997(3)	N(3)–Fe(1)–N(7)	95.0(2)	N(10)–Fe(2)–N(4)	165.6(2)
Fe(1)–N(7)	2.001(3)	N(9)–Fe(1)–N(7)	90.7(2)	N(5)–Fe(2)–N(4)	76.8(1)
Fe(1)–N(8)	2.007(3)	N(3)–Fe(1)–N(8)	84.5(2)	N(12)–Fe(2)–N(4)	98.0(1)
Fe(1)–N(2)	2.024(3)	N(9)–Fe(1)–N(8)	89.6(2)	N(11)–Fe(2)–N(4)	102.2(1)
Fe(1)–N(1)	2.131(2)	N(7)–Fe(1)–N(8)	90.4(2)	N(6)–Fe(2)–N(4)	74.7(1)
Fe(2)–N(10)	2.099(3)	N(3)–Fe(1)–N(2)	94.3(2)	N(19)–Fe(3)–N(20)	90.5(1)
Fe(2)–N(5)	2.146(3)	N(9)–Fe(1)–N(2)	91.3(2)	N(19)–Fe(3)–N(21)	89.5(1)
Fe(2)–N(12)	2.164(3)	N(7)–Fe(1)–N(2)	92.6(2)	N(20)–Fe(3)–N(21)	90.7(1)
Fe(2)–N(11)	2.183(3)	N(8)–Fe(1)–N(2)	176.8(2)	N(19)–Fe(3)–N(15)	93.5(1)
Fe(2)–N(6)	2.188(3)	N(3)–Fe(1)–N(1)	83.0(1)	N(20)–Fe(3)–N(15)	85.7(1)
Fe(2)–N(4)	2.263(3)	N(9)–Fe(1)–N(1)	92.3(1)	N(21)–Fe(3)–N(15)	175.4(1)
Fe(3)–N(19)	1.953(3)	N(7)–Fe(1)–N(1)	171.4(1)	N(19)–Fe(3)–N(14)	91.6(1)
Fe(3)–N(20)	1.955(3)	N(8)–Fe(1)–N(1)	97.7(1)	N(20)–Fe(3)–N(14)	177.7(1)
Fe(3)–N(21)	1.963(3)	N(2)–Fe(1)–N(1)	79.2(1)	N(15)–Fe(3)–N(14)	93.3(1)
Fe(3)–N(15)	1.966(3)	N(10)–Fe(2)–N(5)	95.6(2)	N(19)–Fe(3)–N(13)	171.7(1)
Fe(3)–N(14)	1.976(2)	N(10)–Fe(2)–N(12)	90.3(2)	N(22)–Fe(4)–N(24)	91.9(2)
Fe(3)–N(13)	2.095(2)	N(5)–Fe(2)–N(12)	173.6(2)	N(22)–Fe(4)–N(18)	93.0(1)
Fe(4)–N(22)	2.097(3)	N(10)–Fe(2)–N(11)	90.4(2)	N(24)–Fe(4)–N(18)	91.5(2)
Fe(4)–N(24)	2.100(3)	N(5)–Fe(2)–N(11)	93.6(1)	N(24)–Fe(4)–N(17)	172.4(2)
Fe(4)–N(18)	2.107(3)	N(12)–Fe(2)–N(11)	83.9(2)	N(18)–Fe(4)–N(17)	93.5(1)
Fe(4)–N(17)	2.124(3)	N(10)–Fe(2)–N(6)	94.3(2)	N(18)–Fe(4)–N(23)	172.6(2)
Fe(4)–N(23)	2.142(3)	N(5)–Fe(2)–N(6)	96.3(1)	N(17)–Fe(4)–N(23)	88.9(1)
Fe(4)–N(16)	2.280(3)	N(12)–Fe(2)–N(6)	85.6(1)		
$[Fe_2$(1,3-tpbd)$(DMF)_6](ClO_4)_4$ (**2**)					
Fe(1)–O(1)	2.075(2)	O(1)–Fe(1)–O(3)	89.45(8)	O(1)–Fe(1)–N(3)	177.19(8)
Fe(1)–O(2)	2.112(2)	O(1)–Fe(1)–O(2)	90.84(8)	O(3)–Fe(1)–N(3)	89.44(8)
Fe(1)–O(3)	2.110(2)	O(3)–Fe(1)–O(2)	97.45(8)	O(2)–Fe(1)–N(3)	86.74(8)
Fe(1)–N(1)	2.312(2)	O(1)–Fe(1)–N(2)	90.65(8)	N(2)–Fe(1)–N(3)	92.03(8)
Fe(1)–N(2)	2.152(2)	O(3)–Fe(1)–N(2)	95.89(8)	O(1)–Fe(1)–N(1)	105.90(7)
Fe(1)–N(3)	2.174(2)	O(2)–Fe(1)–N(2)	166.58(7)	O(3)–Fe(1)–N(1)	163.39(7)
N(3)–Fe(1)–N(1)	75.51(7)	O(2)–Fe(1)–N(1)	88.79(7)	N(2)–Fe(1)–N(1)	77.98(7)
$[Zn_2$(1,3-tpbd)$(CH_3CN)_2(SO_3CF_3)_2(H_2O)](SO_3CF_3)_2$ (**4**)					
Zn(1)–N(1)	2.350(5)	N(1)–Zn(1)–N(2)	78.3(2)	N(4)–Zn(2)–N(5)	79.0(2)
Zn(1)–N(2)	2.032(5)	N(1)–Zn(1)–N(3)	78.9(2)	N(4)–Zn(2)–N(6)	79.1(2)
Zn(1)–N(3)	2.046(5)	N(2)–Zn(1)–N(3)	156.1(2)	N(5)–Zn(2)–N(6)	152.3(2)
Zn(1)–N(60)	2.078(5)	N(1)–Zn(1)–O(12)	93.1(2)	N(4)–Zn(2)–O(11)	97.6(2)
Zn(1)–O(1)	2.243(5)	N(2)–Zn(1)–O(12)	89.0(2)	N(5)–Zn(2)–O(11)	105.7(2)
Zn(1)–O(12)	2.242(4)	N(3)–Zn(1)–O(12)	99.4(2)	N(6)–Zn(2)–O(11)	93.9(2)

Table 1. (*Continued*)

Zn(2)–N(4)	2.346(4)	O(1)–Zn(1)–O(12)	173.4(2)	O(11)–Zn(2)–O(21)	167.3(2)
Zn(2)–N(5)	2.024(4)	N(2)–Zn(1)–O(1)	89.2(2)	N(4)–Zn(2)–O(21)	88.3(2)
Zn(2)–N(6)	2.021(5)	O(1)–Zn(1)–N(1)	92.7(2)	N(5)–Zn(2)–O(21)	86.5(2)
Zn(2)–N(70)	2.104(5)	N(3)–Zn(1)–O(1)	84.8(2)	N(70)–Zn(2)–O(11)	90.1(2)
Zn(2)–O(11)	2.122(4)	N(60)–Zn(1)–O(1)	86.5(2)	N(5)–Zn(2)–N(70)	100.2(2)
Zn(2)–O(21)	2.578(4)	N(60)–Zn(1)–N(1)	178.9(2)	N(70)–Zn(2)–O(21)	84.0(2)
		N(2)–Zn(1)–N(60)	100.9(2)	N(6)–Zn(2)–O(21)	76.1(2)
		N(3)–Zn(1)–N(60)	101.7(2)	N(70)–Zn(2)–N(4)	172.3(2)
		N(60)–Zn(1)–O(12)	87.7(2)	N(6)–Zn(2)–N(70)	99.3(2)
$[Zn_2(1,3\text{-tpbd})Cl_4]$ (**5**)					
Zn(1)–N(11)	2.046(6)	N(11)–Zn(1)–N(21)	120.1(3)	N(41)–Zn(2)–N(31)	124.6(3)
Zn(1)–N(21)	2.055(6)	N(11)–Zn(1)–Cl(1)	116.6(2)	N(41)–Zn(2)–Cl(3)	105.6(2)
Zn(1)–Cl(1)	2.248(2)	N(21)–Zn(1)–Cl(1)	113.0(2)	N(31)–Zn(2)–Cl(3)	120.9(2)
Zn(1)–Cl(2)	2.305(2)	N(11)–Zn(1)–Cl(2)	98.3(2)	N(41)–Zn(2)–Cl(4)	99.1(2)
Zn(1)–N(1)	2.646(2)	N(1)–Zn(1)–N(11)	71.7(2)	N(2)–Zn(2)–N(31)	72.9(2)
Zn(2)–N(31)	2.066(7)	N(21)–Zn(1)–Cl(2)	100.8(2)	N(31)–Zn(2)–Cl(4)	98.6(2)
Zn(2)–N(41)	2.042(7)	Cl(1)–Zn(1)–Cl(2)	103.5(1)	Cl(3)–Zn(2)–Cl(4)	102.4(1)
Zn(2)–Cl(4)	2.314(3)	Zn(1)–Cl(1)–O(1)	89.9(2)	Zn(2)–Cl(3)–O(1)	110.2(2)
Zn(2)–Cl(3)	2.259(3)	C(16)–N(11)–Zn(1)	122.0(6)	C(32)–N(31)–Zn(2)	117.6(6)
Zn(2)–N(2)	2.594(3)	N(1)–Zn(1)–Cl(1)	94.8(2)	N(2)–Zn(2)–Cl(3)	97.4(2)
$[CuZn(1,3\text{-tpbd})Cl_4]$ (**7**)					
Zn(1)–N(11)	2.03(2)	N(11)–Zn(1)–N(21)	145.4(4)	N(41)–Cu(1)–N(51)	143.4(4)
Zn(1)–N(21)	2.04(2)	N(11)–Zn(1)–Cl(2)	95.1(3)	N(41)–Cu(1)–Cl(3)	102.2(3)
Zn(1)–Cl(2)	2.307(4)	N(21)–Zn(1)–Cl(2)	96.4(3)	N(51)–Cu(1)–Cl(3)	104.0(3)
Zn(1)–Cl(1)	2.333(3)	N(11)–Zn(1)–Cl(1)	99.2(3)	N(41)–Cu(1)–Cl(4)	96.7(3)
Zn(1)–N(1)	2.37(2)	N(21)–Zn(1)–Cl(1)	109.6(3)	N(51)–Cu(1)–Cl(4)	97.9(3)
Cu(1)–N(41)	2.04(2)	Cl(2)–Zn(1)–Cl(1)	103.3(2)	Cl(3)–Cu(1)–Cl(4)	110.0(2)
Cu(1)–N(51)	2.06(2)	N(11)–Zn(1)–N(1)	76.9(4)	N(41)–Cu(1)–N(2)	74.6(3)
Cu(1)–Cl(3)	2.279(3)	N(21)–Zn(1)–N(1)	77.2(4)	N(51)–Cu(1)–N(2)	74.1(3)
Cu(1)–Cl(4)	2.284(3)	Cl(2)–Zn(1)–N(1)	150.8(3)	Cl(3)–Cu(1)–N(2)	105.2(3)
Cu(1)–N(2)	2.499(2)	Cl(1)–Zn(1)–N(1)	105.6(3)	Cl(4)–Cu(1)–N(2)	144.8(3)
$[Cu_2(1,3\text{-tpbd})_2(H_2O)_2](ClO_4)_4$ (**8**)					
Cu(1)–N(1)	2.074(3)	N(3)–Cu(1)–N(2)	164.8(2)	N(2)–Cu(1)–N(1)	82.4(2)
Cu(1)–N(2)	1.986(3)	N(3)–Cu(1)–N(5)[a]	98.4(2)	N(3)–Cu(1)–O(1)	89.4(2)
Cu(1)–N(3)	1.976(3)	N(2)–Cu(1)–N(5)[a]	96.8(2)	N(3)–Cu(1)–N(1)	83.5(2)
Cu(1)–N(5)	2.000(3)	N(5)[a]–Cu(1)–N(1)	157.4(2)	N(2)–Cu(1)–O(1)	87.0(2)
Cu(1)–O(1)	2.286(3)	N(5)[a]–Cu(1)–O(1)	104.1(2)	N(1)–Cu(1)–O(1)	98.5(1)
$[Cu_2(2,6\text{-tpcd})(H_2O)(Cl)](ClO_4)_2\cdot 2H_2O$ (**9**)					
Cu(1)–O(2)	1.993(2)	O(2)–Cu(1)–N(5)	94.3(1)	N(3)–Cu(2)–N(2)	159.1(1)
Cu(1)–N(5)	2.003(2)	O(2)–Cu(1)–N(6)	99.3(1)	N(3)–Cu(2)–N(1)	82.9(1)
Cu(1)–N(6)	2.013(2)	N(5)–Cu(1)–N(6)	163.8(1)	N(2)–Cu(2)–N(1)	81.9(1)
Cu(1)–N(4)	2.064(2)	O(2)–Cu(1)–N(4)	176.8(1)	N(3)–Cu(2)–O(1)	96.0(1)
Cu(1)–O(1)	2.153(2)	N(5)–Cu(1)–N(4)	82.9(1)	N(2)–Cu(2)–O(1)	96.5(1)
Cu(2)–N(3)	1.996(2)	N(6)–Cu(1)–N(4)	83.6(1)	N(1)–Cu(2)–O(1)	84.0(1)
Cu(2)–N(2)	2.007(2)	O(2)–Cu(1)–O(1)	94.9(1)	N(3)–Cu(2)–Cl(1)	97.8(1)
Cu(2)–N(1)	2.076(2)	N(5)–Cu(1)–O(1)	94.9(1)	N(2)–Cu(2)–Cl(1)	96.6(1)
Cu(2)–O(1)	2.106(2)	N(6)–Cu(1)–O(1)	92.6(1)	N(1)–Cu(2)–Cl(1)	176.7(1)
Cu(2)–Cl(1)	2.280(1)	N(4)–Cu(1)–O(1)	83.7(1)	O(1)–Cu(2)–Cl(1)	99.1(1)

[a] $-x+1$, $-y+1$, $-z+1$.

and uncoordinated perchlorate anions, four acetonitrile solvent molecules and one water molecule. There are only minor structural differences between the two dinuclear cations. In each cation, the intramolecular Fe···Fe separation is 7.488(1) and 7.697(2) Å, respectively. The 1,3-tpbd ligand coordinates each iron(II) center through two pyridine nitrogen atoms and one aliphatic amine nitrogen atom, displaying N_{amine}–Fe–$N_{pyridine}$ angles averaging ca. 81° to accommodate the five-membered chelate rings.

As has been observed previously for Fe^{II}TPA complexes, the Fe–N_{amine} distances ranging from 2.095(2) to 2.280(3) Å are characteristically longer than the Fe–$N_{pyridine}$ bond lengths of 1.966(3) to 2.188(3) Å.[26–28] Three *fac*-coordinated acetonitrile molecules occupy the remaining coordination sites to complete the slightly distorted octahedral coordination geometry around each iron(II) center, with Fe–N–C angles ranging from 166.7(3) to 177.1(3)° and the Fe–N distances ranging from 1.953(3) to 2.183(3) Å. These

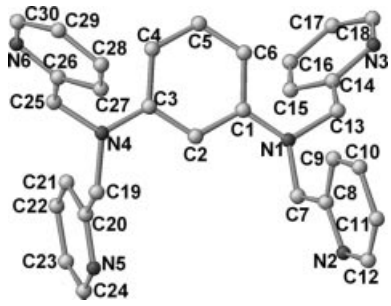

Figure 2. Molecular structure of 1,3-tpbd; hydrogen atoms are omitted for clarity.

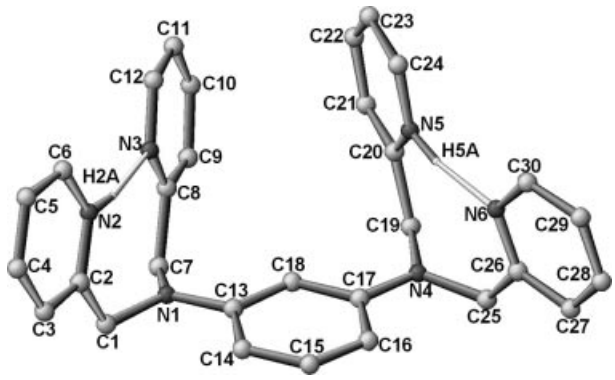

Figure 3. Molecular structure of the cation of $[1,3\text{-tpbdH}_2](ClO_4)_2$; only hydrogen atoms involved in hydrogen bonding are shown.

shorter Fe–N distances indicate that the nitrile groups of the acetonitrile solvent molecules are strongly coordinated to the iron(II) center. Intermolecular π···π interactions (ca. 3.675 Å) exist between C26–C27–C28–C29–C30–N6 and C56–C57–C58–C59–C60–N15 of adjacent pyridine rings from two independent dinuclear cations.

Furthermore, a second iron(II) complex, $[Fe_2(1,3\text{-tpbd})(DMF)_6](ClO_4)_4$ (**2**), was prepared. The molecular structure of the cation of complex **2** is shown in Figure 5 (crystal structure data and refinement parameters, bond lengths and angles are presented in Table 2 and Table 1). Compound **2** crystallizes with half a molecule per crystallographic independent unit of the unit cell, the other half is generated by the crystallographic twofold axis of the space group. Each iron(II) center lies in a distorted N_3O_3 octahedral coordination environment. The equatorial plane around Fe(1) comprises two pyridyl nitrogen atoms [N(2) and N(3)] from the *fac*-coordinated 1,3-tpbd ligand and two oxygen atoms [O(1) and O(2)] from coordinated DMF solvent molecules. Apical positions are occupied by the tertiary amine nitrogen N(1) of 1,3-tpbd and oxygen atom O(3) from a third DMF solvent molecule. The $Fe–N_{pyridine}$ bond lengths [2.152(2)–2.174(2) Å] are characteristically shorter than those of $Fe–N_{amine}$ [2.312(2) Å] and the *cis* $N_{pyridine}–Fe–N_{pyridine}$ angles [92.03°] are entirely consistent with

Table 2. Crystallographic data for 1,3-tpbd ligand and compounds **1**, **2** and **4**.

Compound	1,3-tpbd	$[1,3\text{-tpbdH}_2](ClO_4)_2$	**1**	**2**	**4**
Empirical formula	$C_{31}H_{32}N_6O$	$C_{66}H_{69}Cl_4N_{15}O_{16}$	$C_{46}H_{53}Cl_4Fe_2N_{14}O_{16.5}$	$C_{24}H_{35}Cl_2FeN_6O_{11}$	$C_{40}H_{39}F_{12}N_9O_{13}S_4Zn_2$
M_r	504.63	1470.16	1319.52	710.33	1340.78
Temperature [K]	193(2)	200(2)	100(2)	200(2)	293(2)
Radiation (λ [Å])	0.71073	0.71073	0.71073	0.71073	0.71073
Crystal size [mm]	$0.48\times0.32\times1.48$	$0.8\times0.6\times0.6$	$0.25\times0.21\times0.07$	$0.8\times0.8\times0.4$	$0.62\times0.50\times0.42$
Crystal system	triclinic	monoclinic	monoclinic	monoclinic	orthorhombic
Space group	$P\bar{1}$ (no. 2)	$P2_1/c$ (no. 14)	$P2_1$ (no. 4)	$C2/c$ (no. 15)	$Pna2_1$ (no. 33)
a [Å]	8.0703(10)	21.818(2)	14.532(2)	34.813(4)	25.712(2)
b [Å]	13.2071(17)	19.862(2)	23.015(2)	11.056(2)	9.569(1)
c [Å]	14.379(2)	16.294(2)	17.284(2)	19.807(2)	21.901(2)
α [°]	64.833(15)	90	90	90	90
β [°]	81.997(16)	102.656(2)	93.12(1)	121.515(2)	90
γ [°]	88.423(15)	90	90	90	90
V [Å^3]	1372.7(3)	6889.1(8)	5772(1)	6499(2)	5388.5(9)
Z	2	4	4	8	4
$\rho_{calcd.}$ [g cm^{-3}]	1.221	1.417	1.518	1.452	1.653
μ [mm^{-1}]	0.077	0.251	0.767	0.692	1.154
F(000)	536	3064	2716	2952	2712
Scan range θ [°]	2.78 to 28.05	1.64 to 28.30	3.32 to 27.10	1.97 to 28.31	2.27 to 27.00
Index ranges	$-9\le h\le9$	$-29\le h\le28$	$-18\le h\le18$	$-46\le h\le46$	$-32\le h\le32$
	$-17\le k\le16$	$-26\le k\le26$	$-29\le k\le29$	$-14\le k\le14$	$-12\le k\le12$
	$-18\le l\le18$	$-21\le l\le21$	$-22\le l\le22$	$-26\le l\le26$	$-27\le l\le27$
Reflections collected	12413	81510	140656	37816	12077
Unique reflections	6069	16875	25407	7966	11763
R_{int}	0.0469	0.0513	0.0542	0.0431	0.0342
Data/restraints/parameters	6069/0/356	16875/42/933	25407/41/1536	7966/45/433	11763/3/730
Goodness-of-fit on F^2	1.042	1.032	1.026	1.056	0.990
R_1, wR_2 [$I>4\sigma(I)$]	0.0511, 0.1290	0.0707, 0.1843	0.0412, 0.0818	0.0460, 0.1192	0.0577, 0.0944
R_1, wR_2 (all data)	0.0847, 0.1464	0.1153, 0.2218	0.0617, 0.0883	0.0709, 0.1308	0.1128, 0.1130
Flack parameter[60]	–	–	0.009(8)	–	–0.02(2)
Largest diff. peak/hole [e·Å^{-3}]	0.262, –0.205	1.107, –0.771	0.689, –0.707	0.688, –0.846	0.373, –0.375

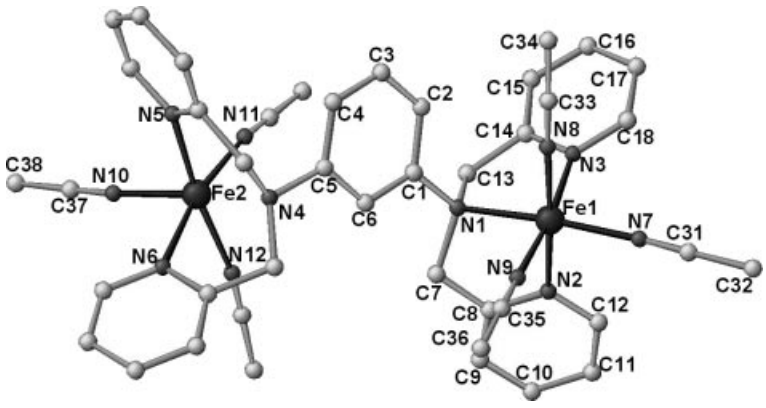

Figure 4. Molecular structure of the cation of $[Fe_2(1,3\text{-tpbd})(CH_3CN)_6](ClO_4)_4 \cdot 2CH_3CN \cdot 0.5H_2O$ (**1**); hydrogen atoms and solvent molecules are omitted for clarity.

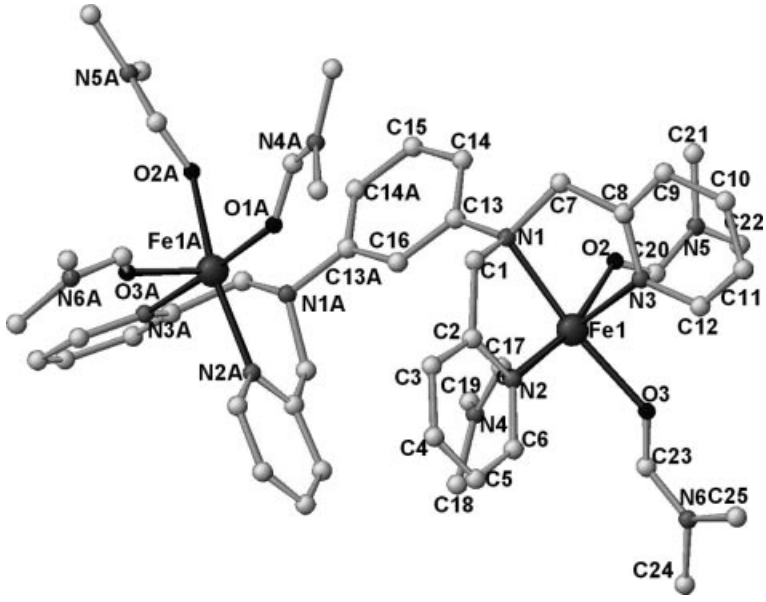

Figure 5. Molecular structure of the cation of $[Fe_2(1,3\text{-tpbd})(DMF)_6](ClO_4)_4$ (**2**); hydrogen atoms are omitted for clarity.

those found in **1**. The Fe–O_{DMF} distances [2.075(2) to 2.112(2) Å] and the average *cis*-coordinated angles [O–Fe–O 92.58°] indicate that the DMF molecules are strongly coordinated to the iron(II) center. The Fe···Fe separation of 6.962 Å is shorter than in **1**, probably a consequence of the stronger π···π interaction (ca. 3.596 Å) between the two pyridine rings (C2–C3–C4–C5–C6–N2 and C2A–C3A–C4A–C5A–C6A–N2A) each from a different tridentate end of the 1,3-tpbd molecule.

Both iron(II) complexes were found to only react slowly with dioxygen, however much faster with hydrogen peroxide. Preliminary kinetic studies of both oxidation reactions indicated complex reaction mechanisms that could not be elucidated. Most likely this is a consequence that 1,3-tpbd is not an innocent ligand and is also involved in the oxidation reactions (see below). Furthermore, efforts to isolate reaction products from these oxidations, such as the according iron(III) complexes described above, were unsuccessful. In contrast with 1,4-tpbd as a ligand only polymeric iron(II) complexes were obtained.[19] With *N*,*N*-bis(2-pyridylmethyl)-aniline (phdpa), the half ligand system of 1,3-tpbd, a 2:1 ligand/metal ion ratio was observed, however, no crystal structures were reported.[20]

Nickel Complexes: Reacting $[Ni(DMF)_6](ClO_4)_2$ with 1,3-tpbd under anaerobic conditions in a glove box led to the nickel(II) analogue of **2**, $[Ni_2(1,3\text{-tpbd})(DMF)_6](ClO_4)_4$ (**3**). Crystals suitable for X-ray crystallography were grown and isolated. Compound **3** crystallizes with nearly identical cell parameters as **2** (Table 2), but the structure of **3** is much better described in the monoclinic space group *C*2 (**3**) than *C*2/*c* (**2**). Accordingly, the systematic absences for the glide plane in *C*2/*c* for **3** are not observed, whereas for **2** these systematic absence conditions are fulfilled absolutely so that the structure of **2** is described correctly in *C*2/*c*. However, a description of the structure of **3** in *C*2/*c* is possible but leads to a significant increase of the R_1 value from 10 to 16%. Therefore; even if it can be assumed from the cell parameters that **2** and **3** are isostructural, the crystal structure of **3** here is presented in the lower symmetric space group *C*2. A Figure of the molecular structure of the cation of **3** as

well as crystal structure data and refinement parameters, bond lengths and angles are presented in the Supporting Information.

The asymmetric unit of complex **3** comprises two crystallographically independent "half" cation units and four ClO_4^- anions, of which three are disordered. The full contents of the unit cell is generated by applying symmetry operations to the asymmetric unit cell. As the structure of **3** is very similar to that of **2** and the calculations might be performed as well in the centrosymmetric space group *C*2/*c* the final absolute structure parameter is relatively high. The two crystallographically independent $[Ni_2(1,3\text{-tpbd})(DMF)_6]^{2+}$ cations of **3** differ only marginally with regard to their bond lengths and angles.

Zinc Complexes: In investigating redox-active metal complexes of iron and copper it is useful to study in comparison complexes with nonredox active centers such as zinc. Copper(II) ions can be substituted by zinc(II) ions and additionally show quite similar coordination behavior. Such zinc(II) complexes themselves can show interesting reaction properties, for example they can be used to hydrolyze diribonucleoside monophosphate diesters.[29] However, in contrast to our expectations the synthesis of a zinc(II) complex of 1,3-tpbd turned out to be more difficult than the synthesis of the according copper(II) complexes. Mixing zinc(II) perchlorate and 1,3-tpbd in alcoholic solution, immediately led to white gelatinous-like precipitates that could not be (re)crystallized. Only after a large number of experiments (applying different conditions), we obtained crystals of the zinc(II) complex $[Zn_2(1,3\text{-tpbd})(CH_3CN)_2(SO_3CF_3)_2(H_2O)](SO_3CF_3)_2$ (**4**) with triflate as a counter anion. The molecular structure of the cation of **4** in Figure 6 shows an unsymmetric di-zinc unit, both ions linked by the *m*-phenylenediamine group and a triflate ion giving an intramolecular Zn···Zn distance of 6.007(1) Å, which is much shorter than in those complexes that are only bridged by 1,3-tpbd. However, it is close to the Cu···Cu distance [5.873(1) Å] in the analogous complex $[Cu_2(1,3\text{-tpbd})(H_2O)_2(ClO_4)_3](ClO_4)$ with an additional perchlorate- in-

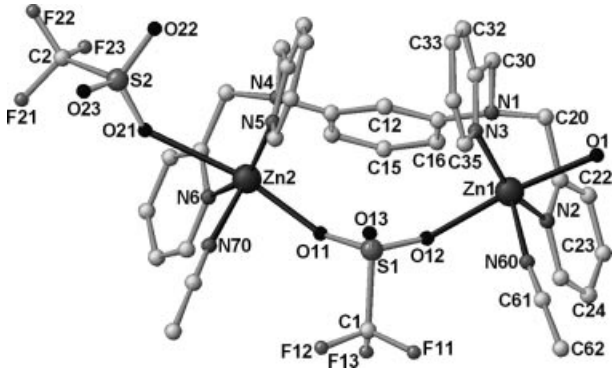

Figure 6. Molecular structure of the cation of $[Zn_2(1,3\text{-tpbd})(CH_3CN)_2(SO_3CF_3)_2(H_2O)](SO_3CF_3)_2$ (**4**). Hydrogen atoms are omitted for clarity.

Table 3. Crystallographic data for compounds **5**–**9**.

Compound	**5**	**7**	**8**	**9**
Empirical formula	$C_{30}H_{30}Cl_4N_6OZn_2$	$C_{30}H_{28}Cl_4CuN_6Zn$	$C_{60}H_{64}Cl_4Cu_2N_{12}O_{20}$	$C_{31}H_{35}Cl_3Cu_2N_6O_{12}$
M_r	763.14	743.29	1542.11	917.08
Temperature [K]	173(2)	173(2)	293(2)	200(2)
Radiation (λ [Å])	0.71073	0.71073	0.71073	0.71073
Crystal size [mm]	0.20 × 0.10 × 0.10	0.30 × 0.20 × 0.20	0.65 × 0.50 × 0.32	0.25 × 0.35 × 0.2
Crystal system	monoclinic	monoclinic	monoclinic	triclinic
Space group	$P2_1/n$ (no. 14)	$P2_1$ (no. 4)	$P2_1/n$ (no. 14)	$P\bar{1}$ (no. 2)
a [Å]	9.177(2)	8.600(2)	10.859(1)	10.495(1)
b [Å]	27.304(6)	13.002(3)	22.660(2)	12.184(2)
c [Å]	12.287(3)	13.690(3)	13.072(1)	14.442(2)
α [°]	90	90	90	93.880(1)
β [°]	91.79(2)	103.24(3)	94.54(1)	95.284(1)
γ [°]	90	90	90	94.411(1)
V [Å^3]	3077.1(2)	1490.1(5)	3206.5(5)	1828.3(3)
Z	4	2	2	2
$\rho_{calcd.}$ [g cm^{-3}]	1.647	1.657	1.597	1.666
μ [mm^{-1}]	1.943	1.910	0.916	1.453
F(000)	1552	754	1588	936
Scan range θ [°]	2.68 to 26.33	2.56 to 33.67	2.08 to 27.00	1.68 to 28.31
Index ranges	$-11 \le h \le 11$	$-10 \le h \le 0$	$-1 \le h \le 13$	$-13 \le h \le 13$
	$-34 \le k \le 0$	$-4 \le k \le 16$	$-28 \le k \le 1$	$-15 \le k \le 16$
	$0 \le l \le 15$	$-17 \le l \le 16$	$-16 \le l \le 16$	$-18 \le l \le 19$
Reflections collected	6543	3407	8527	16512
Unique reflections	6256	3196	7002	8570
R_{int}	0.1193	0.0611	0.0214	0.0363
Data/restraints/parameters	6256/0/388	3196/1/379	7002/5/507	8570/0/518
Goodness-of-fit on F^2	1.014	1.757	1.016	0.892
R_1, wR_2 [$I > 4\sigma(I)$]	0.0610, 0.1181	0.0569, 0.2133	0.0500, 0.0993	0.0388, 0.0848
R_1, wR_2 (all data)	0.1834, 0.1670	0.0704, 0.2198	0.0932, 0.1155	0.0693, 0.0923
Flack parameter[60]	–	–	–	–
Largest diff. peak/hole [e Å^{-3}]	0.829, –0.790	1.361, –1.294	0.459, –0.450	0.720, –0.651

stead of the triflate-bridge (crystal structure data and refinement parameters, selected bond lengths and angles are presented in Table 3 and Table 1).[1]

The coordination geometry around Zn1 is best described as distorted octahedral. The equatorial plane around the zinc(II) center is occupied by three N-donor atoms of the meridional capping ligand 1,3-tpbd (N1, N2 and N3). Apical positions are occupied by O12 of the bridging triflate anion and O1 of a water molecule. The nature of the ligands around Zn2 differs from Zn1 in that a terminal triflate, instead of a water molecule, occupies one of the apical coordination sites. The $N_{pyridine}$–Zn–$N_{pyridine}$ bond angles of 156.1(2)° and 152.3(2)° in **4** are smaller than $N_{pyridine}$–Cu–$N_{pyridine}$ in $[Cu_2(1,3\text{-tpbd})(H_2O)_2](ClO_4)_4\cdot 4H_2O$ [164.5(2)°] apparently owing to the bigger steric hindrance of the triflate ion. Accordingly, both distances of Zn–$N_{pyridine}$ in the range of 2.021(5)–2.046(5) Å and Zn–N_{amine} at 2.350(5) and 2.346(4) Å are longer than those in $[Cu_2(1,3\text{-tpbd})(H_2O)_2](ClO_4)_4\cdot 4H_2O$ [av. Cu–$N_{pyridine}$ 1.969(5) Å; Cu–N_{amine} 2.089(5) Å]. This also applies for the distance of the acetonitrile substituent [Zn–$N_{C\equiv N}$ av. 2.091(5) Å] instead of water [Cu–O_w 1.985(5) Å] at the fourth equatorial site. A triflate anion bridges the two zinc(II) centers via O11 and O12 [Zn1–O12 2.242(4) Å and Zn2–O11 2.122(4) Å]. The structure is "capped" at the apical positions by a water molecule [Zn1–O1 2.243(5) Å] for Zn1 and by a terminal triflate anion [Zn2–O21 2.578(4) Å]. To the best of our knowledge there is only one further example of a crystal structure containing a bridging triflate anion linking two zinc(II) ions found in the Cambridge Crystallographic Database.[30] Efforts to obtain crystals of the (1,3-tpbd)copper(II) triflate analogue failed so far. Furthermore, using 1,4-tpbd as a ligand only a mononuclear zinc complex, $[ZnCl_2(1,4\text{-tpbd})]$, was obtained and its crystal structure has been reported.[19]

In contrast to the according copper(II) complexes, complex **4** is diamagnetic and can be studied in solution by ^1H NMR spectroscopy. Four types of pyridine proton resonances are found in the range 7.4–8.6 ppm (see Exp. Sect.). These four proton resonances represent four symmetry equivalent sets of the pyridine protons found in the complex. Two triplets and two doublets are formed by the splitting of each pyridine proton by its adjacent proton(s). The splitting scheme is depicted in Figure 7. H_a is split into a doublet by H_b (J = 5 Hz), and H_d is split into a doublet by H_c (J = 8 Hz). Proton H_a is assigned to the downfield doublet, and H_d as the upfield doublet. H_b is split by both H_a (J = 6 Hz) and H_c (J = 7 Hz) to form a triplet, and H_c is split by both H_b (J = 7 Hz) and H_d (J = 8 Hz) to form a triplet. H_c is assigned to the downfield triplet, and H_b is assigned to the upfield triplet. The assignments of H_c and H_b are based on greater stabilisation of electron withdrawal in the *para* position, compared to the *meta* position, and previous assignments of pyridine protons in related compounds.[31]

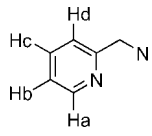

Figure 7. NMR assignment in complex **1**, **2** and **4**.

Heterodinuclear Zinc(II) and Copper(II) Complexes: After achieving the synthesis of a zinc(II) complex as well as the previously reported copper(I) and copper(II) complexes with the ligand 1,3-tpbd, it was obvious that we should try to prepare a heterodinuclear zinc(II) copper(II) complex as a model complex for the enzyme superoxide dismutase (CuZnSOD).[32–38] However, mixing stoichiometric amounts of 1,3-tpbd together with zinc(II) and copper(II) chloride did not lead to the isolation of pure $[CuZn(1,3\text{-tpbd})Cl_4]$, but instead to a mixture of the three dinuclear complexes: $[Zn_2(1,3\text{-tpbd})Cl_4]$ (**5**), $[Cu_2(1,3\text{-tpbd})Cl_4]$ (**6**) and $[CuZn(1,3\text{-tpbd})Cl_4]$ (**7**). Structural characterization of all three complexes was achieved by picking individual crystals (that were different in color) from the reaction mixture. The molecular structure of **5** is shown in Figure 8 and that of **7** in Figure 9 (crystal structure data and refinement parameters, bond lengths and angles are presented in Table 3 and Table 1).

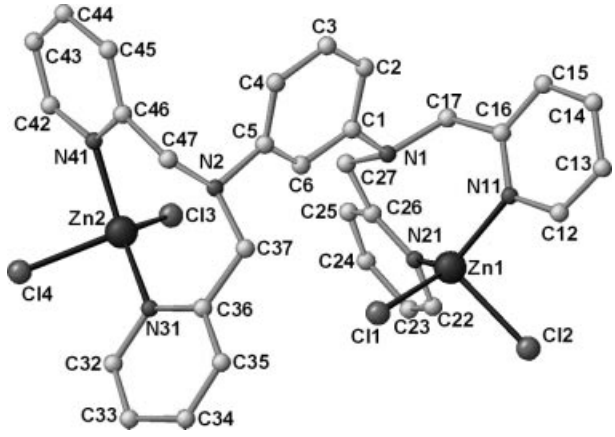

Figure 8. Molecular structure of $[Zn_2(1,3\text{-tpbd})Cl_4]$ (**5**); hydrogen atoms are omitted for clarity.

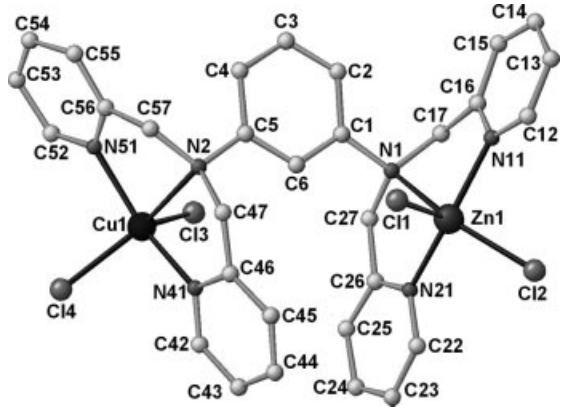

Figure 9. Molecular Structure of $[CuZn(1,3\text{-tpbd})Cl_4]$ (**7**); hydrogen atoms are omitted for clarity.

The crystal structure of $[Cu_2(1,3\text{-tpbd})Cl_4]$ (**6**) has been obtained previously in a different study and crystallographic details will be published elsewhere.[13] Due to the fact that here X-ray crystallography measurements do not allow the differentiation between zinc and copper ions, the presence of the different metal ions was further confirmed by photon-induced X-ray emission spectroscopy of the crystals of **5**, **6** and **7**.

The metal ions are linked through the 1,3-phenylenediamine group leading to an intramolecular Zn···Zn distance of 6.925 Å for **5** and Cu···Zn separation of 6.849 Å for **7**, both of them shorter than the Cu···Cu distance of 7.434 Å for **6**. In **5**, the zinc(II) ions are pentacoordinate by three nitrogen atoms of the 1,3-tpbd ligand and two chloride ions, with the following distances: Zn1–Cl1 2.248(2), Zn1–Cl2 2.305(2), average Zn1–$N_{pyridine}$ 2.050(6) and Zn1–N_{amine} 2.646(2) Å. Considering such weak N_{amine} ligation to zinc(II) ions, the coordination geometry around Zn1 and Zn2 can be described as distorted trigonal bipyramidal. The axial positions of the coordination sphere around Zn1 are occupied by N1 and Cl2 and the equatorial plane of the ZnN_3Cl_2 unit comprises N11, N22 and Cl1 with Zn1 lying out of the basal plane by 0.2956 Å. Compared to the mononuclear zinc(II) 1,4-tpbd complex with Zn–$N_{pyridine}$ average distance 2.14(1) Å and Zn–N_{amine} 2.26(1) Å, where the Zn–$N_{pyridine}$ distance is significantly longer and the Zn–N_{amine} distance is significantly shorter than in **5**.[19] In **7**, both coordination geometries around the copper(II) and zinc(II) centers are close to trigonal bipyramidal with N41 and N51 occupying the axial positions around Cu1 and N11 and N21 occupying the axial positions of Zn1. Similar to complex **5**, the three nitrogen atoms of one tridendate end of the 1,3-tpbd ligand and the metal center to which they are coordinated are almost coplanar, with Cu–$N_{pyridine}$ average distance 2.054(2) and Cu–N_{amine} 2.499(2) Å, Zn–$N_{pyridine}$ average distance 2.034(2) and Zn–N_{amine} 2.370(2) Å. The Cu–Cl distances are very close to each other [2.279(3) and 2.284(3) Å], likewise for the Zn–Cl bonds [2.307(4) and 2.333(3) Å]. The Zn–$N_{pyridine}$ and Cu–$N_{pyridine}$ distances are in accordance to those determined for related mononuclear analogues, in contrast the Zn–N_{amine} and Cu–N_{amine} distances in the mononuclear complexes of 2.142(2) Å and 2.207(6) Å are significantly shorter.[39,40] However, these complexes are complexes with a different ligand to metal cation ratio (one metal ion and two coordinated bispicolylamine ligands) at the amine nitrogen atom and the hydrogen atom is not substituted by an organic group.

"Zinc-Ion-Assisted" Formation of a Dinuclear Copper Complex: During our efforts to prepare model complexes for CuZnSOD described above, we observed a very surprising reaction behavior when stoichiometric mixtures of copper(II) and zinc(II) perchlorate salts were mixed with 1,3-tpbd. Instead of obtaining the heterodinuclear complex, we isolated a new dinuclear copper(II) complex, $[Cu_2(1,3\text{-tpbd})_2(H_2O)_2](ClO_4)_4$ (**8**), in which two copper(II) ions had reacted with two 1,3-tpbd ligand units. The molecular structure of the cation of complex **8** is shown in Figure 10 (crystal structure data and refinement parameters, bond lengths and angles are presented in Table 3 and Table 1).

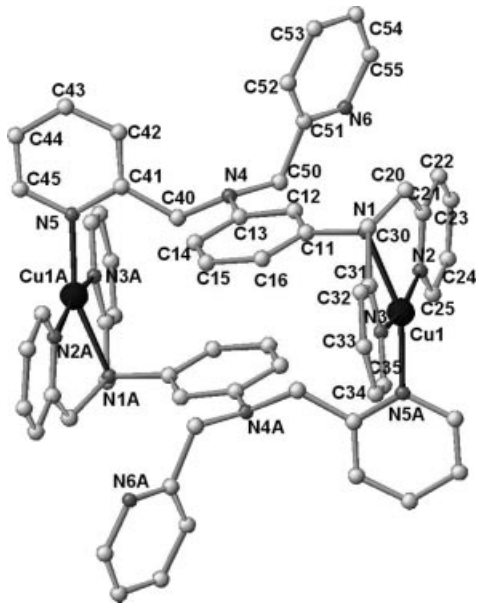

Figure 10. Molecular structure of the cation of $[Cu_2(1,3\text{-tpbd})_2(H_2O)_2](ClO_4)_4$ (**8**); water molecules and hydrogen atoms are omitted for clarity.

Complex **8** is a so called "dimetallocyclophane" and it is interesting to compare its structure with the dinuclear complex, $[Cu_2L'_2(H_2O)_2](ClO_4)_4{\cdot}2H_2O$, obtained previously from an impurity that was formed during the synthesis of 1,3-tpbd.[1] The "impurity" L′ is a derivative of the 1,3-tpbd ligand, missing one pyridyl "arm" (derived from incomplete formation of 1,3-tpbd during synthesis). A schematic presentation of the complex with the "impurity" as ligand in comparison with **8** is shown in Figure 11.

Complex **8** likewise crystallizes with an inversion center located in the middle of the "dimetallocyclophane" core. However, the metal coordination sphere is quite different to that of $[Cu_2L'_2(H_2O)_2](ClO_4)_4{\cdot}2H_2O$. The copper(II) ions in **8** exhibit a "4+1" square-based pyramidal geometry with three nitrogen atoms (N1, N2 and N3) from one tridentate end of 1,3-tpbd in the meridional form, and the pyridine (N5A) from the symmetry-related ligand completing the basal plane, while a water molecule (O1) occupies the apical site. In **8** the tertiary amine (N4A) from the symmetry-related ligand is not bound to the copper(II) center with a long distance of 4.472 Å, while the corresponding nitrogen (N2) as a secondary amine is coordinated to the copper(II) center with a bond length of 2.071(2) Å in the corresponding $[Cu_2L'_2(H_2O)_2](ClO_4)_4{\cdot}2H_2O$ complex.

The two pyridyl "arms" from the same tertiary amine are *trans* to one another [N2–Cu1–N3 164.8(2)°], [Cu1–N2 1.986(3), Cu1–N3 1.976(3) Å]. However, the corresponding two pyridyl nitrogen atoms in $[Cu_2L'_2(H_2O)_2](ClO_4)_4{\cdot}2H_2O$ are *cis*-coordinated to copper(II) with a N11–Cu1–N12 angle of 86.2(5)°. In complex **8**, all the Cu–$N_{pyridine}$ lengths are in general slightly shorter than the *trans* Cu–$N1_{amine}$ [2.074(3) Å]. The steric influence of the non-coordinated

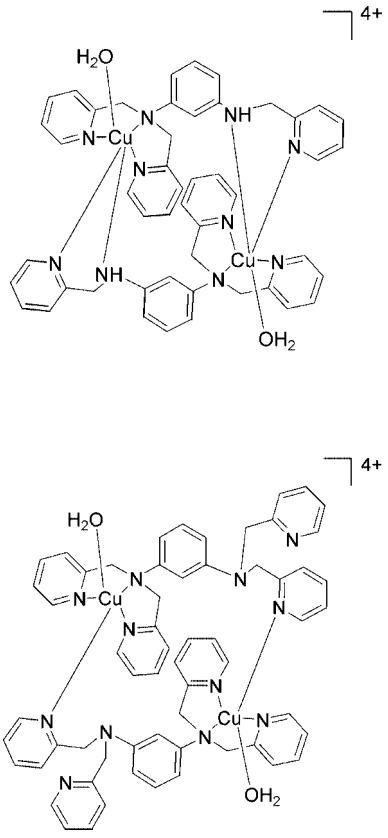

Figure 11. Schematic representation of the complex with the "impurity"L′ as ligand (top) in comparison to **8** (bottom).

pyridine ring results in the different coordination geometry and an intramolecular distance of Cu···Cu [8.820(1) Å] which is 1.3 Å longer than that of $[Cu_2L'_2(H_2O)_2](ClO_4)_4 \cdot 2H_2O$.

The finding that **8** forms despite the presence of zinc(II) ions is extremely surprising due to the results described above that zinc(II) can substitute copper(II) ions perfectly well in complexes of the ligand 1,3-tpbd. Furthermore, **8** can also be prepared if only a small amount (e.g. 5%) of zinc(II) ions are present. This result clearly suggests that zinc(II) ions should not be necessarily present and that it should be possible to synthesize **8** by mixing copper(II) perchlorate and 1,3-tpbd in a one to one stoichiometric ratio (Figure 12) because the reaction in a stoichiometric ratio of one (1,3-tpbd) to two $Cu(ClO_4)_2$ affords the dinuclear copper(II) complex $[Cu_2(1,3\text{-tpbd})(H_2O)_2(ClO_4)_3](ClO_4)$ that has been structurally characterized previously.[1]

However, in contrast a series of experiments showed that **8** cannot be prepared under aerobic conditions without the presence of zinc(II) ions. For example a mixture of 1,3-tpbd and one equivalent of copper(II) perchlorate in methanol/H_2O, acetonitrile or DMF exposed to air caused the effect that the green solutions rapidly started to turn to a deep-red color within a day.

Such a phenomenon has precedence with other related *m*-phenylendiamine derivatives where radical reactions were observed during oxidation reactions.[41–43] A possible mechanism (shown in Figure 13) can be postulated according to these previous findings (most likely an oxygen atom

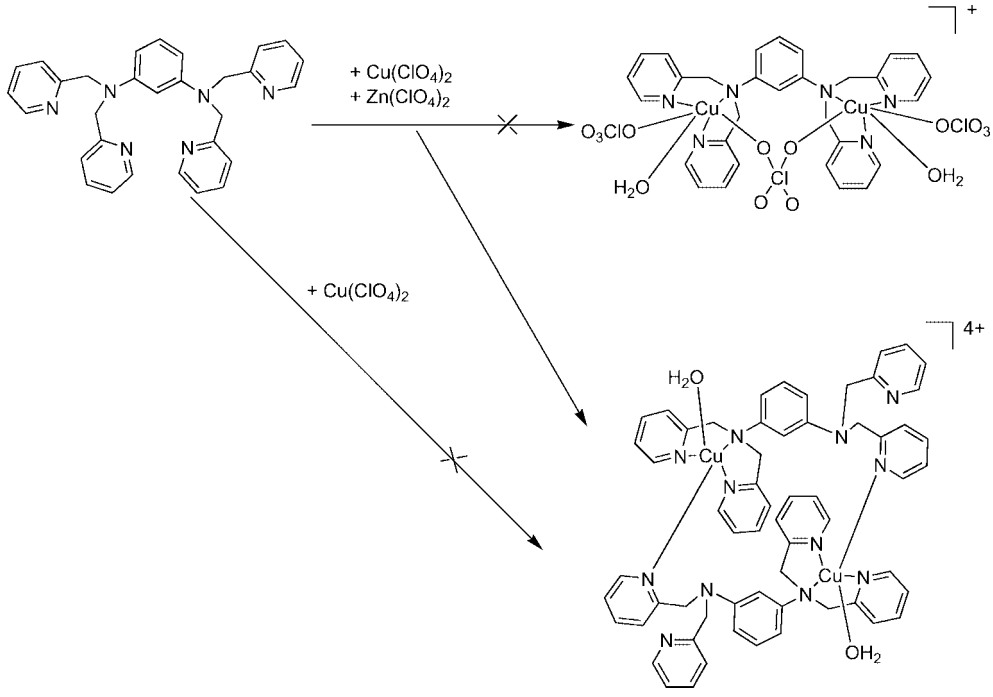

Figure 12. Scheme of reactions observed during the "zinc-assisted" formation of **8**.

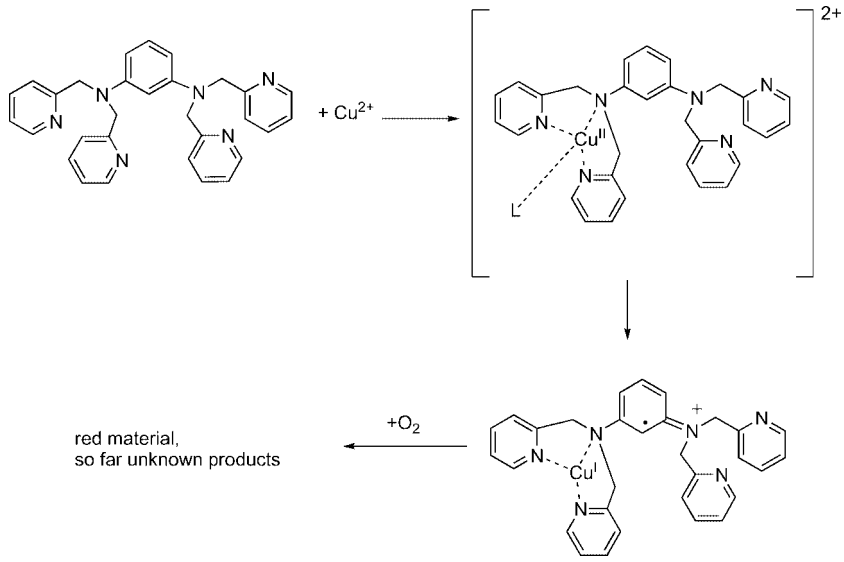

Figure 13. Possible reaction scheme for the formation of an oxidation product of 1,3-tpbd.

reacts with the benzene ring of the 1,3-tpbd ligand).[42] Unfortunately, all our efforts to identify this "red" material in order to ascertain whether 1,3-tpbd has been modified have been unsuccessful (only oily dark red reaction mixture products could be obtained so far).

However, this part of the postulated mechanism of ligand oxidation could readily explain the zinc(II) assisted crystallization of **8**. If enough copper(II) ions are present the formation of the radical intermediate shown in Figure 13 will be suppressed because both coordination sites are blocked with the copper(II) ions and dinuclear copper(II) complexes such as $[Cu_2(1,3\text{-tpbd})(H_2O)_2(ClO_4)_3]$-$ClO_4$ can be easily prepared.

If nonredox-active zinc(II) ions are present they will (as outlined above) coordinate to 1,3-tpbd as well. Most likely – and not for an obvious reason – they seem to prefer coordination only to one of the ligand sites as observed previously with the 1,4-tpbd derivative as ligand (see above), where even the crystal structure of this 1:1 complex was reported.[19] Then, the other coordination site will be filled with a copper(II) ion and in a consecutive reaction the zinc(II) ion will now be substituted by a copper(II) ion already coordinated to another 1,3-tpbd ligand molecule. Thus the zinc(II) ion will be liberated and can again interact with a different 1,3-tpbd ligand molecule [which would also explain why stoichiometric amounts of zinc(II) ions are not necessary]. Once complex **8** is formed, radical oxidations are again suppressed, and therefore allow the facile synthesis and isolation of complex **8**.

In our efforts to get a better understanding of the assumed ligand-oxidation processes we also reinvestigated the oxidation of the dinuclear 1,3-tpbd copper(I) complex with dioxygen described previously.[1] In the past this reaction has been studied in methanol, a solvent less suitable for stabilizing reactive intermediates such as copper "dioxygen adduct" complexes.[1] In our current experiments using more suitable solvents such as acetone we observed spectral changes that indicate the formation of a peroxido copper complex (even at ambient temperature), however, so far all efforts to isolate or to characterize this species in a pure form were unsuccessful.

As a complimentary means to obtain insights into the structure and energetics of possible dioxygen adduct complexes we performed quantum chemical calculations at the B3LYP/TZVP level of density functional theory. We optimized the structures of three isomers, i.e. the (η^2:η^2)-peroxido, the bis-μ-oxido, and the *trans*-(η^1:η^1)-peroxido species. These calculations corroborate the interpretation of a side-on-bound (η^2:η^2)-peroxido species as the most stable complex formed. According to the quantum chemical results, the bis-μ-oxido species is 3.2 kcal/mol less stable, followed by the *trans*-peroxido species, which is 12.1 kcal/mol less stable than the side-on-bound peroxido isomer. Key parameters of the optimized structures are shown in Figure 14.

So far our efforts to isolate and characterize the final oxidation product(s) have been unsuccessful. A possible product that could arise from an intramolecular ligand hydroxylation similar to oxidation reactions observed previously for related systems[11] would lead to a phenol ligand shown in Figure 1 (R = H). Therefore we synthesized a derivative of this ligand (R = CH_3) from 2,6-diamino-*p*-cresol dihydrochloride[44] and 2-chloromethylpyridine hydrochloride. The copper(II) complex was obtained easily when copper(II) perchlorate was mixed with the ligand and crystals suitable for crystallographic characterization could be isolated. The crystal structure of $[Cu_2(2,6\text{-tpcd})(H_2O)(Cl)]$-$(ClO_4)_2 \cdot 2H_2O$ (**9**) is shown in Figure 15 (crystal structure data and refinement parameters, bond lengths and angles are presented in Table 3 and Table 1). The coordinated chloride ion is a consequence of the usage of the protonated ligand (isolation as the hydrochloride salt). The H atoms of water solvent molecules were derived from a difference Fou-

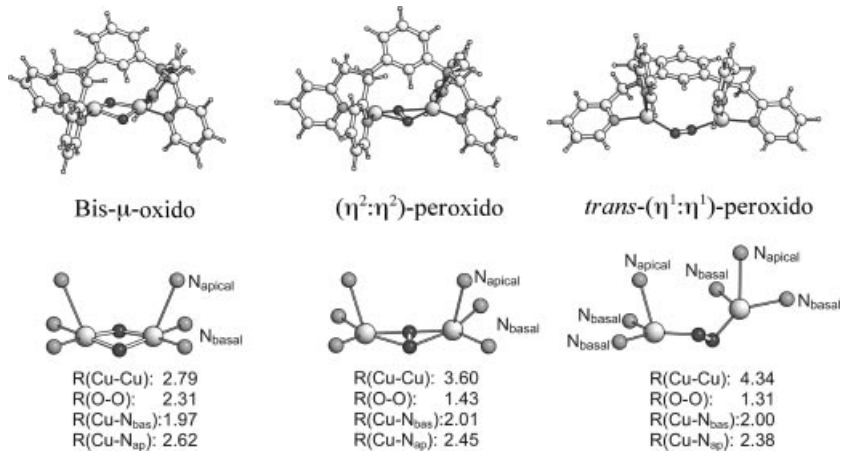

Figure 14. Calculated structures of the dioxygen copper adduct complex of 1,3-tpbd.

rier map and isotropically refined. **9** crystallizes with one coordinated and two additional water solvent molecules per unit.

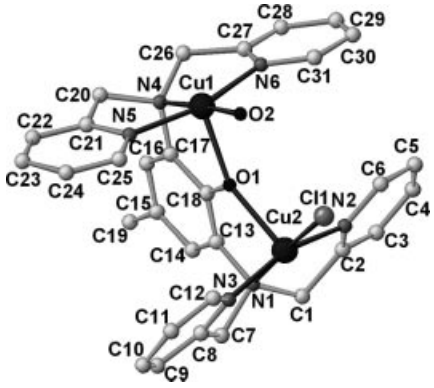

Figure 15. Molecular structure of the cation of $[Cu_2(2,6\text{-tpcd})(H_2O)(Cl)](ClO_4)_2$ (**9**).

In **9** both copper(II) ions are "4+1" coordinated forming a distorted square-pyramidal geometry. The basal plane consists of two pyridine nitrogen atoms (N2 and N3), the amine nitrogen N1 and the chloride anion Cl1 while the apical plane consists of the phenol oxygen atom O1. The distance between both copper(II) ions is 4.027 Å. Interestingly the distance Cu1–O1 with 2.153(1) Å is slightly longer than the corresponding distance Cu2–O1 [2.106(2) Å].

Parallel to our work, Karlin and co-workers investigated the reactivity of a dinuclear copper(I) complex with a nearly identical ligand (PD′OH) (Figure 1, R = *tert*-butyl). Besides selective DNA interactions of this complex[15] they furthermore reported in that regard a very interesting hydroxylation reaction of nitriles to aldehyde and cyanide during oxidation. A hydroperoxido complex has been postulated as reactive species in these reactions.[16]

Conclusions

1,3-tpbd is a versatile ligand that can be used successfully to coordinate two metal ions in close proximity. While the nickel complex shows normal coordination behavior, redox active metal centers such as iron or copper ions demonstrate that 1,3-tpbd is a non-innocent ligand. Interestingly 1,3-tpbd does not coordinate iron(III) ions, instead protonation of the ligand is preferred. Oxidations of iron(II) complexes or copper(I) complexes of 1,3-tpbd led to reaction product mixtures that could not be characterized so far. Theoretical calculations support the formation of a dinuclear side-on peroxido copper complex during the reaction of the copper(I) complex with dioxygen. Intramolecular ligand hydroxylation might occur during the oxidation reaction, however, could not be proved experimentally. The possible reaction product, a phenolate-bridged derivative of the 1,3-tpbd complex could be synthesized in an independent way. Most interestingly is the reaction if only one equivalent of copper(II) salt is reacted with one equivalent of 1,3-tbpd. Under aerobic conditions a red product was formed after a short while, suggesting ligand oxidation. However, this reaction could be suppressed completely in the presence of zinc ions. Here $[Cu_2(1,3\text{-tpbd})_2(H_2O)_2](ClO_4)_4$ a so called "dimetallocyclophane" formed.

Experimental Section

General Remarks: All chemicals were purchased from commercial sources and used as received.

CAUTION! *The perchlorate salts used in this study are potentially explosive and should be handled with care.*

Physical Measurements: Elemental analyses were carried out with a Carlo Erba 1106 using a Mettler Toledo UMX-2. NMR spectra were recorded with a 400 MHz Bruker-Aspect 2000/3000. IR spectra were recorded with a Bruker Optics IFS25.

Ligand Synthesis: The ligand *N*,*N*,*N*′,*N*′-tetrakis(2-pyridylmethyl)-benzene-1,3-diamine (1,3-tpbd) was synthesized according to litera-

ture procedures.[1] Slow evaporation of a methanol solution of 1,3-tpbd in a glove box afforded single crystals suitable for X-ray diffraction studies.

2,6-Bis[bis(2-pyridylmethyl)amino]-*p*-cresol (2,6-tpcd): A solution of sodium hydroxide (4.18 g, 0.1050 mol) in water (30 mL) was added dropwise with stirring to a mixture of 2,6-diamino-*p*-cresole·2HCl[44] (2 g, 0.0095 mol) and 2-(chloromethyl)pyridine hydrochloride (7.82 g, 0.0475 mol) in 5 mL H_2O under inert conditions. The crude product was recrystallized several times from acetone and 0.5 g (0.001 mol) 10.5% 2,6-tpcd were obtained. ^{1}H NMR ($CDCl_3$/TMS, 400 MHz): δ = 8.48 (m, 4 H, pyr-H_a), 7.48 (m, 4 H, pyr-H_c), 7.45 (m, 8 H, pyr-H_b/H_d), 7.39 (s, 2 H, Ar-H), 4.75 (s, 8 H, –CH_2–), 2.15 (s, 3 H, -CH_3) ppm.

$[H_4(1,3\text{-tpbd})_2](ClO_4)_4\cdot(CH_3CN)_3$: A solution of iron(III) perchlorate hydrate (141.7 mg, 0.4 mmol) in water (3 mL) was added to a solution of 1,3-tpbd (95.2 mg, 0.2 mmol) in CH_3OH (7 mL). The reaction mixture (a brown suspension) was stirred for 1 h at room temperature and filtered. The precipitate was dissolved in CH_3CN (5 mL) and allowed to stand at room temperature for 2 d affording yellow block-shaped crystals suitable for X-ray diffraction analysis. $C_{66}H_{69}Cl_4N_{15}O_{16}$(1470.16): calcd. C 53.92, H 4.73, N 14.29; found C 53.78, H 4.94, N 14.51.

$[H_4(1,3\text{-tpbd})_2](SO_3CF_3)_4$: The complex was obtained in a similar way as for the perchlorate salt described above, however, for this compound no analytical data were collected. The crystal structure and data are reported in the Supporting Information.

Synthesis of Complexes

$[Fe_2(1,3\text{-tpbd})(CH_3CN)_6](ClO_4)_4\cdot(CH_3CN)_2\cdot(H_2O)_{0.5}$ (1) and $[Fe_2(1,3\text{-tpbd})(DMF)_6](ClO_4)_4$ (2): Complexes **1** and **2** were synthesized by the same procedure in a glove box differing only by the different solvents used. $Fe(ClO_4)_2\cdot H_2O$ (101.9 mg; 0.4 mmol) and 1,3-tpbd (95.2 mg, 0.2 mmol) were dissolved in 10 mL of CH_3CN or DMF. The resulting clear, light-brown solution was stirred for 30 min at room temperature followed by vapor diffusion with diethyl ether (20 mL) at –11 °C. Nearly colorless square crystals of **1** and light yellow plate crystals of **2** suitable for X-ray diffraction analysis were grown after three weeks. Yield: 161 mg (0.12 mmol, 61%) for **1** and 159 mg (0.11 mmol, 56%) for **2**. $C_{46}H_{53}Cl_4Fe_2N_{14}O_{16.50}$ (1319.52) (**1**): calcd. C 41.87, H 4.05, N 14.86; found C 41.74, H 3.99, N 14.69. $C_{24}H_{35}Cl_2FeN_6O_{11}$ (710.33)(**2**): calcd. C 40.58, H 4.97, N 11.83; found C 40.65, H 4.84, N 11.87. ^{1}H NMR (CD_3CN, 400 MHz): for **1**: δ = 9.78 (d, J_{HH} = 1.9 Hz, 4 H, pyr-H_a), 8.97 (t, $^3J_{HH}$ = 7.7 Hz, 4 H, pyr-H_c), 8.55 (t, $^3J_{HH}$ = 5.5 Hz, 4 H, pyr-H_b), 8.49 (d, J_{HH} = 7.4 Hz, 4 H, pyr-H_d), 8.07 (t, $^3J_{HH}$ = 14.6 Hz, 1 H, Ar-H), 7.32 (s, 1 H, Ar-H), 7.26 (dd, J_{HH} = 6.99 Hz, 2 H, Ar-H), 6.00 (s, 8 H, –CH_2–) ppm; (CD_3CN, 400 MHz) for **2**: δ = 8.40 (d, 4 H, pyr-Ha), 8.00 (s, 1 H, DMF-H), 7.59 (t, 4 H, pyr-Hc), 7.05–7.16 (t/d, 8 H, pyr-Hb/–Hd), 6.70 (t, 1 H, Ar-H), 5.85–5.97 (s/d, 3 H, Ar-H), 4.61 (s, 8 H, –CH_2–), 2.71–2.87 (s, 36 H, DMF-CH_3) ppm.

$[Ni_2(1,3\text{-tpbd})(DMF)_6](ClO_4)_4$ (3): Similar to the above procedure for **1** and **2**, this complex was synthesized by adding a solution of $[Ni(DMF)_6](ClO_4)_2$[45] in DMF to a solution of 1,3-tpbd in DMF under the inert conditions of a glove box. Crystals suitable for X-ray diffraction analysis were obtained by slow diffusion of diethyl ether into the solution. $C_{48}H_{70}Cl_4N_{12}Ni_2O_{22}$ (1426.38): calcd. C 40.42, H 4.95, N 11.78; found C 39.77, H 4.48, N 11.60. UV/Vis (DMF): λ_{max} = 612, 774, 937 nm. The crystal structure and data are reported in the Supporting Information.

$[Zn_2(1,3\text{-tpbd})(CH_3CN)_2(SO_3CF_3)_2(H_2O)](SO_3CF_3)_2$ (4): Zinc triflate (154 mg, 0.42 mmol) was added to a solution of 1,3-tpbd (100 mg, 0.21 mmol) in acetonitrile under an inert atmosphere. The solution was allowed to stir at room temperature for a further 2 h. The solvent was removed in vacuo and dichloromethane (5 mL) was added to the residual oil. Diethyl ether (20 mL) was added until the solution was slightly turbid. The vessel was placed in the freezer compartment of a fridge and within 3 d, large transparent blocks of 4 formed. IR (Nujol mull): $\tilde{\nu}$ 3631 (w), 3629 (w), 3627 (w), 3549 (w), 3434 (w), 3245 (m), 3120 (m), 2972 (s), 2948 (s), 2885 (s), 2845 (s), 2726 (m), 2676 (m), 2416 (w), 2394 (w), 2317 (m), 2288 (m), 2211 (w), 2038 (w), 1923 (w), 1610 (m), 1582 (m), 1456 (s), 1376 (s), 1287 (s), 1246 (s), 1167 (s), 1105 (m), 1031 (s), 957 (m), 901 (m), 850 (m), 817 (m), 774 (m), 726 (m), 696 (m), 634 (m), 574 (m), 544 (m), 517 (m), 472 (w) cm^{-1}. ^{1}H NMR (CD_3CN, 300 MHz): δ = 8.60 (d, $^3J_{HH}$ = 4.9 Hz, 4 H, pyr-H_a), 8.10 (t, $^3J_{HH}$ = 7.5 Hz, 4 H, pyr-H_c), 7.63 (t, J_{HH} = 6.0 Hz, 4 H, pyr-Hb), 7.44 (d, $^3J_{HH}$ = 7.9 Hz, 4 H, pyr-H_d), 6.90 (t, $^3J_{HH}$ = 8.3 Hz, 1 H, Ar-H), 6.33 (dd, $^3J_{HH}$ = 1.9 Hz, 1 H, 8.7 Hz, Ar-H), 5.96 (s, 1 H, Ar-H), 4.60 (s, 8 H, –CH_2–).

$[Zn_2(1,3\text{-tpbd})Cl_4]\cdot H_2O$ (5), $[Cu_2(1,3\text{-tpbd})Cl_4]$ (6), $[CuZn(1,3\text{-tpbd})Cl_4]$ (7): Slow evaporation of an aqueous methanolic solution of a stoichiometric mixture of $ZnCl_2$, $CuCl_2$ and 1,3-tpbd led to a mixture of yellow and two different green-colored crystals suitable for X-ray diffraction analysis.

$[Cu_2(1,3\text{-tpbd})_2(H_2O)_2]\cdot(ClO_4)_4\cdot 2H_2O$ (8): A methanolic suspension of 1,3-tpbd (95.2 mg, 0.2 mmol) was added to an aqueous methanol solution of $Cu(ClO_4)_2\cdot 6H_2O$ (64.1 mg, 0.2 mmol) and $Zn(ClO_4)_2\cdot 6H_2O$ (74.4 mg, 0.2 mmol). The mixture was stirred for 2 h, filtered and allowed to slowly evaporate at room temperature. Large green blocks formed within 48 h. A single-crystal X-ray diffraction analysis was performed and the structure of the green crystals was determined to be $[Cu_2(1,3\text{-tpbd})(OH_2)_2](ClO_4)_4$. That no zinc ions were present at all was further confirmed by photon-induced X-ray emission.

$[Cu_2(2,6\text{-tpcd})(H_2O)(Cl)](ClO_4)_2\cdot 2H_2O$ (9): A suspension of 2,6-tpcd (100 mg, 0.2 mmol) in 5 mL methanol was added to a solution of $Cu(ClO_4)_2\cdot 6\ H_2O$ (148.2 mg, 0.4 mmol) in 5 mL H_2O. The mixture was stirred for 30 min at room temperature and allowed to slowly evaporate at room temperature. Within two days small green needles of **9** suitable for X-ray diffraction analysis were formed.

Computational Methods: Density functional calculations have been performed employing the B3LYP functional[46–49] as implemented in the Turbomole program.[50–52] The TZVP basis set has been employed for all atoms.[53] Solvent effects have partially been included in these calculations employing the COSMO continuum solvent model (dielectric constant for acetone at room temperature: ε = 36.64).[54]

X-ray Crystallographic Studies: X-ray crystallographic data for 1,3-tpbd were collected with a STOE IPDS-diffractometer at 193 K equipped with a low-temperature system (Karlsruher Glastechnisches Werk). Cell parameters were refined by using up to 5000 reflections. A sphere of data (210 frames) was collected with the φ oscillation mode (0.9° frame width; Irradiation times/frame: 7 min.) No absorption corrections were applied. The structures were solved by direct methods in SHELXS97, and refined by using full-matrix least-squares in SHELXL97.[55] The hydrogen atoms were positioned geometrically and all non-hydrogen atoms were refined anisotropically, if not mentioned otherwise. All following data were corrected for Lorentz and polarization effects. Intensity data of **1** were collected with a Bruker-Nonius KappaCCD diffractometer, intensity data for **4** and **8** were collected with a Siemens P4 four circle diffractometer. Absorption effects were corrected either by semi-empirical methods based on multiple scans (**1**)[56] or on the

basis of Psi-scans.[57] The structures were solved by direct methods; full-matrix least-squares refinement was carried out on F^2 using SHELXTL NT 6.12.[58] All non-hydrogen atoms were refined anisotropically. Hydrogen atoms were geometrically positioned except for the hydrogen atoms of the water molecules or aqua ligands the positions of which were derived from a difference Fourier synthesis; their isotropic displacement parameters were tied to those of their corresponding carrier atoms by a factor of 1.2 or 1.5. One of the perchlorate anions of **1** is disordered; two preferred orientations were refined resulting in occupancy factors of 50.1(6) and 49.9(6) %. In **8** both of the two independent perchlorate anions are subjected to disorder. Two preferred orientations refined led to occupancy factors of 72(2) and 28(2)% around Cl1 and 61(2) and 39(2) % around Cl2, respectively.

Intensity data of protonated tpbd, **2**, **3** and **9** were collected with a Siemens SMART CCD 1000 diffractometer by the ω-scan technique collecting a full sphere of data with irradiation times of 10 to 20 s per frame and $\Delta\omega$ ranges between 0.3° and 0.45°. The collected reflections were corrected for absorption effects.[56] All structures were solved by direct methods and refined by least-squares techniques using the SHELX97 programme package.[55] The hydrogen atoms were positioned geometrically and all non-hydrogen atoms were refined anisotropically, if not mentioned otherwise. Further data collection parameters are summarised in Tables 2, 3 and in the Supporting Information.

Intensity data of of **5** and **7** were collected with a Nonius MACH3 diffractometer. Cell parameters were obtained and refined from 25 reflections. Absorption corrections (psi-scans) were applied. The space groups were determined from systematic absences and subsequent least-squares refinement. The structures were solved by direct methods. The parameters were refined with all data by full-matrix-least-squares on F^2 using SHELXL-97.[55] Non-hydrogen atoms were refined with anisotropic thermal parameters. The hydrogen atoms were fixed in idealized positions using a riding model. Scattering factors were taken from the literature.[59] Figures of the molecular structures were obtained using Winray.[61]

CCDC-610594 (for 1,3-tpbd), -610424 (for $[1,3\text{-tpbdH}_2](ClO_4)_2$), -615270 (for **1**), -610425 (for **2**), -610426 (for $[1,3\text{-tpbdH}_2](CF_3SO_3)_2$), -610427 (for **3**), -615271 (for **4**), -611033 (for **5**), -611034 (for **7**), -615272 (for **8**) and -610428 (for **9**) contain the supplementary crystallographic data for this paper. These data can be obtained free of charge from The Cambridge Crystallographic Data Centre via www.ccdc.cam.ac.uk/data_request/cif.

Supporting Information (see also the footnote on the first page of this article): Crystallographic data and selected bond lenghts and angles of $[H_2]1,3\text{-tpbd}](SO_3CF_3)_2$ and **3**.

Acknowledgments

The authors gratefully acknowledge financial support from the Deutsche Forschungsgemeinschaft (DFG). S. P. F. is thankful for a scholarship from the Deutscher Akademischer Austauschdienst (DAAD).

[1] S. Schindler, D. J. Szalda, C. Creutz, *Inorg. Chem.* **1992**, *31*, 2255–2264.
[2] S. P. Foxon, G. R. Torres, O. Walter, J. Z. Pedersen, H. Toftlund, M. Hueber, K. Falk, W. Haase, J. Cano, F. Lloret, M. Julve, S. Schindler, *Eur. J. Inorg. Chem.* **2004**, 335–343.
[3] S. P. Foxon, O. Walter, R. Koch, H. Rupp, P. Müller, S. Schindler, *Eur. J. Inorg. Chem.* **2004**, 344–348.
[4] E. A. Lewis, W. B. Tolman, *Chem. Rev.* **2004**, *104*, 1047–1076.
[5] L. M. Mirca, X. Ottenwaelder, T. D. P. Stack, *Chem. Rev.* **2004**, *104*, 1013–1045.
[6] S. Schindler, *Eur. J. Inorg. Chem.* **2000**, 2311–2326.
[7] L. Q. Hatcher, K. D. Karlin, *J. Biol. Inorg. Chem.* **2004**, *9*, 669–683.
[8] I. Fernández, R. Ruiz, J. Faus, M. Julve, F. Lloret, J. Cano, X. Ottenwaelder, Y. Journaux, M. C. Muñoz, *Angew. Chem. Int. Ed.* **2001**, *40*, 3039–3042.
[9] X. Ottenwaelder, J. Cano, Y. Journaux, E. Rivière, C. Brennan, M. Nierlich, R. Ruiz-Garcia, *Angew. Chem. Int. Ed.* **2004**, *43*, 850–852.
[10] A. Hoffmann, R. van Eldik, *Dalton Trans.* **2003**, 2979–2985.
[11] N. N. Murthy, M. Mahroof-Tahir, K. D. Karlin, *J. Am. Chem. Soc.* **1993**, *115*, 10404–10405.
[12] N. N. Murthy, K. D. Karlin, I. Bertini, C. Luchinat, *J. Am. Chem. Soc.* **1997**, *119*, 2156–2162.
[13] C. J. McKenzie, M. Julve, S. Schindler, unpublished results.
[14] T. N. Sorrell, M. L. Garrity, D. J. Ellis, *Inorg. Chim. Acta* **1989**, *166*, 71–75.
[15] L. Li, K. D. Karlin, S. E. Rokita, *J. Am. Chem. Soc.* **2005**, *127*, 520–521.
[16] L. Li, A. A. Narducci Sarjeant, M. A. Vance, L. N. Zakharov, A. N. Rheingold, E. I. Solomon, K. D. Karlin, *J. Am. Chem. Soc.* **2005**, *127*, 15360–15361.
[17] T. N. Sorrell, C. O'Connor, O. P. Anderson, J. H. Reibenspies, *J. Am. Chem. Soc.* **1985**, *107*, 4199–4206.
[18] T. Buchen, A. Hazell, L. Jessen, C. J. McKenzie, L. Preuss Nielsen, J. Z. Pedersen, D. Schollmeyer, *Dalton Trans.* **1997**, 2697–2704.
[19] A. Hazell, C. J. McKenzie, L. J. Preuss Nielsen, *J. Chem. Soc., Dalton Trans.* **1998**, 1751–1756.
[20] A. Hazell, C. J. McKenzie, L. Preuss Nielsen, *Polyhedron* **2000**, *19*, 1333–1338.
[21] A. Mederos, P. Gili, S. Domínguez, A. Benítez, M. Soledad Palacios, M. Hernández-Padilla, P. Martín-Zarza, M. L. Rodríguez, C. Ruíz-Pérez, F. J. Lahoz, L. A. Oro, F. Brito, J. M. Arrieta, M. Vlassi, G. Germain, *J. Chem. Soc., Dalton Trans.* **1990**, 1477–1491.
[22] E. Y. Tshuva, S. J. Lippard, *Chem. Rev.* **2004**, *104*, 987–1012.
[23] M. Costas, M. P. Mehn, M. P. Jensen, L. Que Jr., *Chem. Rev.* **2004**, *104*, 939–986.
[24] S. V. Kryatov, E. V. Rybak-Akimova, S. Schindler, *Chem. Rev.* **2005**, *105*, 2175–2226.
[25] I. Bernal, I. M. Jensen, K. B. Jensen, C. J. McKenzie, H. Toftlund, J. P. Tuchagues, *J. Chem. Soc., Dalton Trans.* **1995**, 3667–3675.
[26] C. R. Randall, L. Shu, Y.-M. Chiou, K. S. Hagen, M. Ito, N. Kitajima, R. J. Lachicotte, Y. Zang, L. Que Jr., *Inorg. Chem.* **1995**, *34*, 1036–1039.
[27] A. Diebold, K. S. Hagen, *Inorg. Chem.* **1998**, *37*, 215–223.
[28] D. Mandon, A. Nopper, T. Litrol, S. Goetz, *Inorg. Chem.* **2001**, *40*, 4803–4806.
[29] M. Yashiro, H. Kaneiwa, K. Onaka, M. Komiyama, *Dalton Trans.* **2004**, *4*, 605–610.
[30] M. L. Hlavinka, M. J. Mc Nevin, R. Shoemaker, J. R. Hagadorn, *Inorg. Chem.* **2006**, *45*, 1815–1822.
[31] J. B. Mandel, C. Maricondi, B. E. Douglas, *Inorg. Chem.* **1988**, *27*, 2990–2996.
[32] I. Fridovich, *Annu. Rev. Biochem.* **1995**, *64*, 97–112.
[33] D. P. Riley, *Chem. Rev.* **1999**, *99*, 2573–2587.
[34] D. Ghosh, N. Kundu, G. Maity, A. Caneschi, A. Endo, M. Chaudhury, *Inorg. Chem.* **2004**, *43*, 6015–6023.
[35] V. Pelmenschikov, P. E. M. Siegbahn, *Inorg. Chem.* **2005**, *44*, 3311–3320.
[36] H. Ohtsu, S. Itoh, S. Nagatomo, T. Kitagawa, S. Ogo, Y. Watanabe, S. Fukuzumi, *Chem. Commun.* **2000**, 1051–1052.
[37] H. Ohtsu, Y. Shimazaki, A. Odani, O. Yamauchi, W. Mori, S. Itoh, S. Fukuzumi, *J. Am. Chem. Soc.* **2000**, *122*, 5733–5741.
[38] S. Fukuzumi, H. Ohtsu, K. Ohkubo, S. Itoh, H. Imahori, *Coord. Chem. Rev.* **2002**, *226*, 71–80.

[39] Y. Gultneh, A. Raza Khan, D. Blaise, S. Chaudry, B. Ahvazi, B. B. Marvey, R. J. Butcher, *J. Inorg. Biochem.* **1999**, *75*, 7–18.
[40] M. Palaniandavar, R. J. Butcher, A. W. Addison, *Inorg. Chem.* **1996**, *35*, 467–471.
[41] A. Calder, A. R. Forrester, P. G. James, G. R. Luckhurst, *J. Am. Chem. Soc.* **1969**, *91*, 3724–3727.
[42] F. Effenberger, W.-D. Stohrer, K.-E. Mack, F. Reisinger, W. Seufert, H. E. A. Kramer, R. Föll, E. Vogelmann, *J. Am. Chem. Soc.* **1990**, *112*, 4849–4857.
[43] M. M. Wienk, R. A. J. Janssen, *J. Am. Chem. Soc.* **1996**, *118*, 10626–10628.
[44] E. Fromm, R. Ebert, *J. Prakt. Chem.* **1924**, *108*, 75–87.
[45] W. Fee, D. Elholum, A. McPherson, D. Rundle, *Aust. J. Chem.* **1973**, *26*, 1207–1225.
[46] A. D. Becke, *Phys. Rev. A* **1988**, *38*, 3098–3100.
[47] A. D. Becke, *J. Chem. Phys.* **1993**, *98*, 5648–5652.
[48] C. Lee, W. Yang, R. G. Parr, *Phys. Rev. B* **1988**, *37*, 785–789.
[49] P. J. Stephens, F. J. Devlin, C. F. Chabalowski, M. J. Frisch, *J. Phys. Chem.* **1994**, *98*, 11623–11627.
[50] R. Ahlrichs, M. Bär, H. P. Baron, R. Bauernschmitt, S. Becker, M. Ehrig, K. Eichkorn, S. Elliott, F. Furche, F. Haase, M. Häser, C. Hättig, H. Horn, C. Huber, U. Huniar, M. Kattanek, A. Köhn, C. Kölmel, M. Kollwitz, K. May, C. Ochsenfeld, H. Öhm, A. Schäfer, U. Schneider, O. Treutler, K. Tsereteli, B. Unterreiner, M. von Arnim, F. Weigend, P. Weis, H. Weiss, in *Turbomole – Program System for ab initio Electronic Structure Calculations*, version 5.6, University of Karlsruhe, **2002**.
[51] R. Ahlrichs, in: *Encyclopedia Computational Chemistry* (Ed.: P. v. R. Schleyer), Wiley, Chichester, **1998**, pp. 3123–3129.
[52] R. Ahlrichs, M. Bär, M. Häser, H. Horn, C. Kölmel, *Chem. Phys. Lett.* **1989**, *162*, 165–169.
[53] A. Schäfer, C. Huber, R. Ahlrichs, *J. Chem. Phys.* **1994**, *100*, 5829–5835.
[54] A. Klamt, G. Schüürmann, *J. Chem. Soc., Perkin Trans. 2* **1993**, 799–805.
[55] G. M. Sheldrick, *SHELX-97*, University of Göttingen, **1997**.
[56] *SADABS 2.06*, Bruker AXS, Inc., Madison, WI, USA, **2002**.
[57] A. T. C. North, D. C. Phillips, F. S. Matthews, *Acta Crystallogr., Sect. A* **1968**, *24*, 351–359.
[58] *SHELXTL NT 6.12*, Bruker AXS, Inc., Madison, WI, USA, **2002**.
[59] D. T. Cromer, J. T. Waber, in *International Tables for X-ray Crystallography* (Eds.: J. A. Ibers, W. C. Hamilton), Kynoch, Birmingham, **1974**.
[60] H. D. Flack, *Acta Crystallogr., Sect. A* **1983**, *39*, 876–881.
[61] Winray: R. Soltek, University of Heidelberg, **1997**; xpma: L. Zsolnai, University of Heidelberg, **1997**.

Received: October 5, 2006
Published Online: December 4, 2006

